

First Principles Study of Structural and Optical Properties of B₁₂ Isomers

Pritam Bhattacharyya

Department of Physics, Indian Institute of Technology Bombay, Powai, Mumbai 400076, India

Ihsan Boustani

Theoretical and Physical Chemistry, Faculty of Mathematics and Natural Sciences, Bergische Universität, Wuppertal, Gauss Strasse 20, D-42097 Wuppertal, Germany

Alok Shukla

Department of Physics, Indian Institute of Technology Bombay, Powai, Mumbai 400076, India

arXiv:1802.01072v2 [physics.atm-clus] 21 May 2019

Abstract

In this work we undertake a comprehensive numerical study of the ground state structures and optical absorption spectra of isomers of B₁₂ cluster. Geometry optimization was performed at the coupled-cluster-singles-doubles (CCSD) level of theory, employing cc-pVDZ extended basis sets. Once the geometry of a given isomer was optimized, its ground state energy was calculated more accurately at the coupled-cluster-singles-doubles along with perturbative treatment of triples (CCSD(T)) level of theory, employing larger cc-pVTZ basis sets. Thus, our computed values of binding energies of various isomers are expected to be quite accurate. Our geometry optimization reveals eleven distinct isomers, along with their point group, and electronic ground state symmetries. We also performed vibrational frequency analysis on the three lowest energy isomers, and found them to be stable. Therefore, we computed the linear optical absorption spectra of these isomers of B₁₂, employing large-scale multi-reference singles-doubles configuration-interaction (MRSDCI) approach, and found a strong structure-property relationship. This implies that the spectral fingerprints of the geometries can be utilized for optical detection, and characterization, of various isomers of B₁₂. We also explored the stability of the isomer with the structure of a perfect icosahedron, with I_h symmetry. In bulk boron icosahedron is the basic structural unit, but, our vibrational frequency analysis reveals that it is unstable in the isolated form. We speculate that this instability could be due to Jahn-Teller distortion because five-fold degenerate HOMO orbitals in I_h structure are unfilled.

Keywords: MRSDCI; Boron clusters; Optical absorption; CCSD(T)

1. Introduction

Since the eighties, and until now, the structures and energetics of small atomic clusters have been of great interest, both experimentally, and theoretically.[1] Initially, the clusters were considered as a bridge, or an accumulation at nanoscale to solids, but over the years, due to sustained research effort, they have become well established as a separate research discipline. Since then, the exploration and synthesis of structures and energetics of pure atomic clusters has acquired both

Email addresses: pritambhattacharyya01@gmail.com (Pritam Bhattacharyya), boustani@uni-wuppertal.de (Ihsan Boustani), shukla@phy.iitb.ac.in (Alok Shukla)

academic and practical importance. Thereupon, the mass spectra of alkali-metal, non-metal, carbon and boron clusters were investigated as well as the related magic numbers were determined.[1] For example, among the allotropes of carbon, all sp^2 -types are closely related and have been extensively studied: graphene (flat monoatomic sheet of graphite), spherical fullerenes, and nanotubes.[2] Also for boron, carbon's left neighbor in the periodic table, the landscape of fullerene-like possibilities is just beginning to emerge: from small quasi-planar clusters, spherical cages and nanotubes [3], then to borophene (single atom-thin monolayer sheet of boron atoms) [4].

However, the development of non crystalline boron beyond the icosahedral arrangements began in the late eighties with theoretical and experimental studies on small boron clusters. Anderson group [5] carried out the first experimental and theoretical study of bonding and structures in boron cluster ions B_n^+ for ($n \leq 13$) in comparison with the well known closo boron hydrides. Further important study on boron clusters was carried out by Kawai and Weare [6] using Car-Parrinello *ab initio* molecular dynamics simulation. They found that an open 3D structure is more stable than the icosahedral boron. However, Kato *et al.*[7] investigated boron clusters B_n for ($n=8-11$) using *ab initio* molecular orbital theory, and concluded that the most stable clusters have planar or pseudo-planar cyclic structures. The breakthrough in boron cluster research happened in 1997 due to the work of one of us,[8] in which it was discovered that the most stable boron clusters have quasi-planar structures of dovetailed hexagons including the B_{12} cluster. In this work, the so-called Aufbau principle was proposed, according to which highly stable novel structures in form of boron sheets (nowadays called borophene), nanotubes, and spheres can be constructed from only two basic units: pentagonal and hexagonal pyramids B_6 , and B_7 , respectively.[8] These novel structures are different from the conventional allotropes of solid boron.

It is well known that the bulk boron exists in several crystalline phases.[9] The most famous boron solids are the rhombohedral α - B_{12} and β - B_{106} phases with 12 and 106 atoms per unit cells, respectively, The α -rhombohedral phase transforms at 1200 °C into the more stable β -rhombohedral one. Besides the α -tetragonal, and β -tetragonal phases with 190-192 atoms per unit cell, there is a new phase of crystalline boron called orthorhombic γ - B_{28} boron [10], with two B_{12} clusters, and two B_2 pairs in the unit cell, accompanied by a charge transfer as boron boride $(B_2)^{\delta+}(B_{12})^{\delta-}$. Remarkable is the common basic unit cell of all these structures: the B_{12} icosahedron. This regular B_{12} icosahedron operates as a building block for all phases mentioned above. Due to the multi-center covalent inter-atomic bonds between the icosahedra, the electron deficiency is reduced, and the electron distribution saturates the twelve boron atoms in each icosahedron, leading to high stability. However, as soon as this B_{12} icosahedron is separated from the bulk, losing its neighbors, and becoming a free standing cluster, it loses its stability, and flattens to transform into a quasi-planar structure.[8] Based upon molecular orbital occupancies, we argue in this work that this flattening of the $B_{12} - I_h$ icosahedron into the quasi-planar $B_{12} - C_{3v}$ structure could be a consequence of Jahn-Teller distortion.

Given the importance of the B_{12} cluster, in this work, we study all its isomers including the icosahedron, and compute the optical absorption spectra of its most stable isomers. For the purpose, we have utilized standard wave function based first principles quantum chemical methodologies, employing Cartesian Gaussian basis functions. Geometry optimization was carried out using the coupled-cluster-singles-doubles (CCSD) approach, while the optical absorption spectra of various isomers were computed using the multi-reference singles-doubles configuration interaction (MRSDCI) approach, which has been extensively utilized in the group of one of us to study optical properties of conjugated polymers,[11, 12, 13, 14, 15] graphene quantum dots,[16, 17] along with atomic clusters such as those of boron,[18] aluminium,[19] sodium,[20] and magnesium.[21]

2. Theoretical approach and Computational details

2.1. Geometry Optimization

The geometries of various isomers of B₁₂ cluster were optimized using the coupled-cluster singles doubles (CCSD) method, and the cc-pVDZ basis set, as implemented in the Gaussian 09 package.[22] The optimized geometries of all the isomers of B₁₂ cluster are shown in the Fig. 1. The final total ground state energies of various isomers reported in Table 1, were obtained by performing single-point energy calculations at those optimized geometries, using the coupled-cluster singles doubles triples (CCSD(T)) method, and the cc-pVTZ basis set. Thus, the final ground state total energies of various isomers were computed using a higher level of theory, and a larger basis set. One important criteria, i.e., the binding energy per atom which is directly related to the stability of the cluster has been computed using the formula

$$\frac{E_b}{n} = E_1 - \frac{E_n}{n}, \quad (1)$$

where E_1 is the energy of a single boron atom, E_n is the total energy of the cluster, and n is the number of atoms present in the cluster. For boron atom $E_1 = -24.598101$ Hartree was used, obtained using CCSD(T) approach as implemented in Gaussian09 program, employing the cc-pVTZ basis set. Computed binding energies per atom of all the eleven isomers are listed in Table 1.

We have also computed the optical absorption spectra of the three lowest-energy structures, which not only have the highest binding energies, but were also found to be stable from the vibrational frequency analysis.

2.2. Optical Absorption Spectrum

With the aim of understanding structure property relationship, we also computed the optical absorption spectra of three of the lowest energy isomers: (a) B₁₂ - quasi-planar , (b) B₁₂ - double ring, and (c) B₁₂ - chain. In order to compute the optical absorption spectra, we utilized the *ab initio* MRSDCI approach, as implemented in the computer program MELD,[23] and described in recent works on the optical properties of clusters.[18, 19, 20, 21] For the purpose, we utilized the geometries of the isomers (quasi-planar, double ring, and chain) presented in Fig. 1, and the cc-pVDZ basis set, which was also used for geometry optimization. Calculations were initiated by performing the restricted Hartree-Fock calculations, and the resultant orbital set (occupied and virtual), served as the single-particle basis for the CI calculations. Because the orbital basis set was fairly large, the following approximations were employed to truncate it: (a) frozen-core approximation, and (b) removal of high-energy virtual orbitals. Both these approximations are justified on the physical grounds in that the orbitals which are far away from the Fermi level are unlikely to contribute to optical excitations. Nevertheless, we critically examine the influence of these approximations on our results in the following section. After fixing the single-particle basis, the next step involves singles-doubles configuration interaction calculations (SDCI), employing single reference wave functions. Ground and the excited states obtained from these calculations are used to calculate the optical absorption spectrum $\sigma(\omega)$, according to the formula

$$\sigma(\omega) = 4\pi\alpha \sum_i \frac{\omega_{i0} |\langle i | \hat{\mathbf{e}} \cdot \mathbf{r} | 0 \rangle|^2 \gamma^2}{(\omega_{i0} - \omega)^2 + \gamma^2}. \quad (2)$$

Above, ω denotes frequency of the incident light, $\hat{\mathbf{e}}$ denotes its polarization direction, \mathbf{r} is the position operator, α is the fine structure constant, 0 and i denote, respectively, the ground and excited states, ω_{i0} is the frequency difference between those states , and γ is the line width, taken as 0.1 eV, in these calculations. The summation over i in Eq. 2 involves an infinite number of excited states

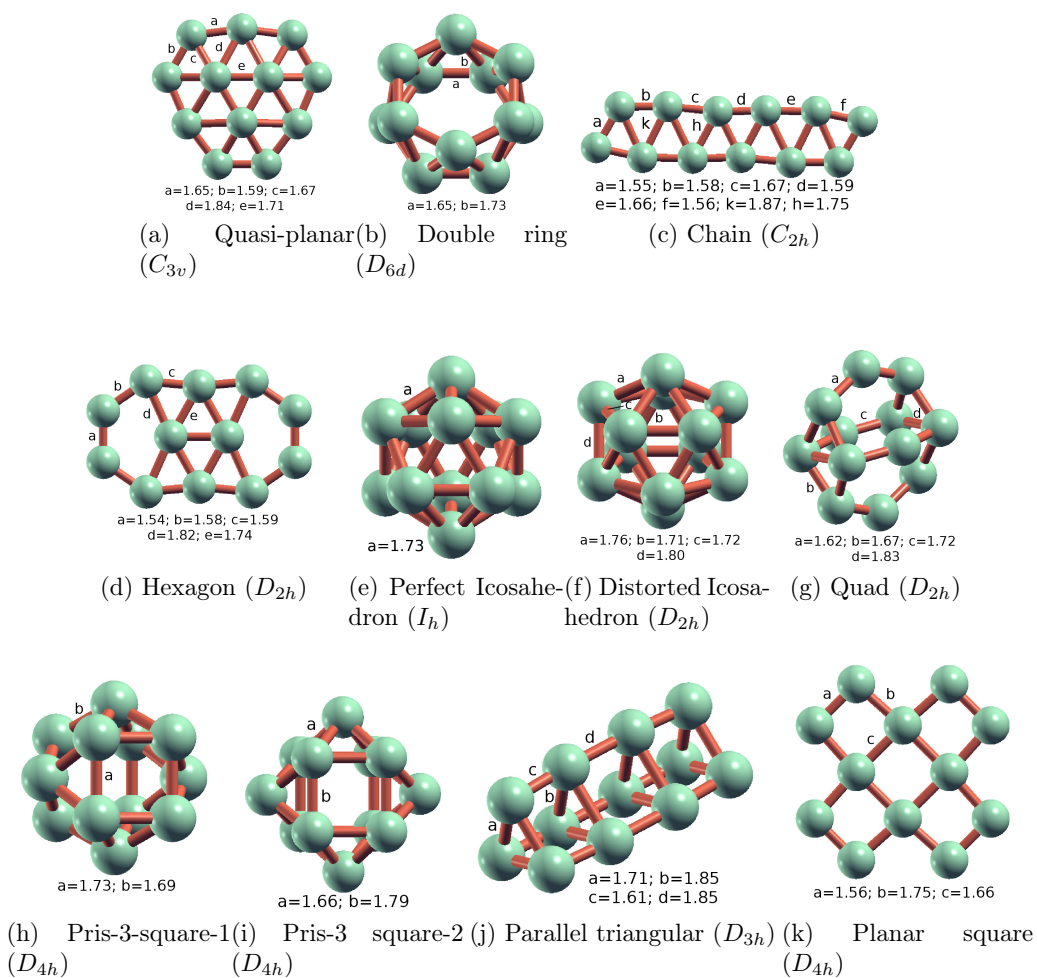


Figure 1: Optimized geometries of various isomers of B_{12} cluster, along with their point group symmetries. Optimizations were performed using CCSD level of theory, and cc-pVDZ basis set, as implemented in the Gaussian 09 package.[22] All isomers have singlet multiplicity, and the bond lengths are in Å unit.

Table 1: All the isomers of B₁₂ cluster have been listed below along with their point group, ground state symmetry, and the ground state energy (in Hartree). Also their relative energy (in eV) with respect to the lowest isomer, i.e., quasi-planar structure is presented in the same table. The correlation energy is the difference of the total energies of the system at the CCSD(T) and the Hartree-Fock levels. In the last column, the binding energy per atom (in eV) is shown to illustrate the stability of the structure.

Isomer	Point group	Ground state symmetry	Ground state energy [†] (Ha)	Relative energy (eV)	Correlation energy per atom (eV)	Binding energy per atom (eV)
Quasi-planar	C _{3v}	¹ A ₁	-297.208187	0.0	2.92	4.60
Double ring	D _{6d}	¹ A ₁	-297.1399191	1.858	3.00	4.45
Chain	C _{2h}	¹ A _g	-297.1029824	2.863	2.92	4.36
Hexagons	D _{2h}	¹ A _g	-297.0853492	3.342	2.97	4.33
Perfect Icosahedron	I _h	¹ A _g	-297.0662229	3.863	3.36	4.28
Distorted Icosahedron	D _{2h}	¹ A _g	-297.077724	3.550	3.35	4.31
Quad	D _{2h}	¹ A _g	-297.0180888	5.173	3.08	4.17
Pris-3-square-1	D _{4h}	¹ A _{1g}	-296.8945639	8.534	3.44	3.89
Pris-3-square-2	D _{4h}	¹ A _{1g}	-296.8192288	10.583	3.29	3.72
Parallel triangular	D _{3h}	¹ A' ₁	-296.7691979	11.945	3.19	3.61
Planar square	D _{4h}	¹ A _{1g}	-296.7132189	13.468	3.36	3.48

[†] Ground state energy was computed using CCSD(T) level of theory and cc-pVTZ basis set.

which are dipole connected to the ground state, while in practice it is restricted to states with excitation energies up to 10 eV. We carefully examine the excited states contributing to the peaks in the absorption spectrum, and the configurations contributing to those are included in the reference set for MRSDCI calculations. A new set of configuration space is generated by considering singles and doubles excitations from the reference set, and the entire procedure is repeated. This process is continued until the calculated absorption spectrum has converged within reasonable limits.[18, 19, 20, 21]

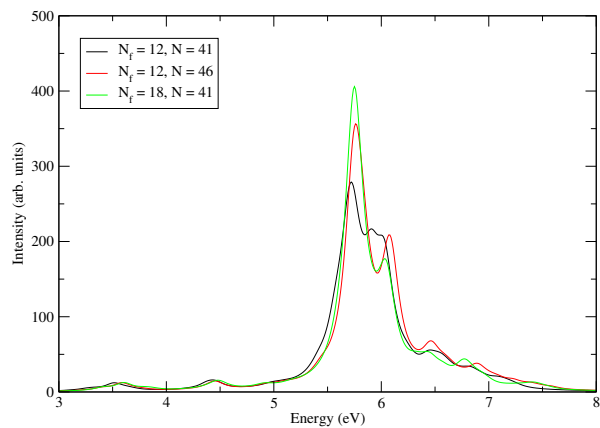
We make a few brief comments about the line width γ occurring in the expression for the optical absorption spectrum (see Eq. 2 above). The line width incorporates all kinds of uncertainties associated with the values of energy levels due to reasons such as: (a) natural line widths, (b) vibrational broadening, because of finite temperature effects, (c) collisional broadening in the gas or liquid phase, (d) impurities and disorder in the samples, and (e) experimental uncertainties. The value $\gamma = 0.1$ eV chosen by us is fairly reasonable, and has been employed in all our past calculations of optical absorption spectra. From the structure of Eq. 2 it is obvious that a smaller value of γ leads to sharper and higher peaks, while a larger value causes the peaks to become broader, and lower in height. Therefore, as per the requirement, one can use any reasonable value of γ .

2.3. Orbital Truncation Scheme

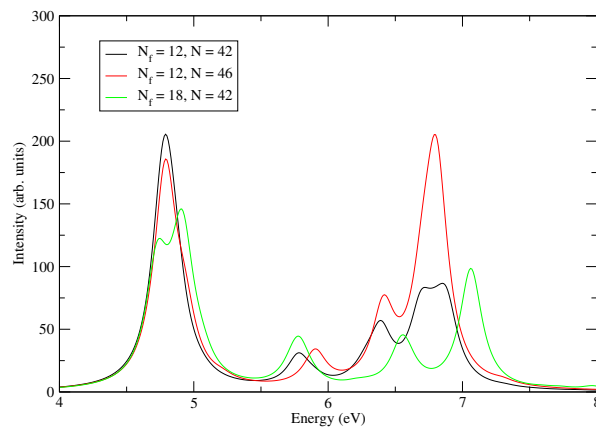
The computational effort in CI calculations grows $\approx N^6$, where N is the total number of active orbitals. Thus, the size of the CI expansion, and hence the computational effort involved proliferates very rapidly with the increasing N . Therefore, the choice of the active orbitals becomes crucial, and determines the feasibility and the quality of the calculations. As discussed earlier, there are two ways to control the value of N : (a) by the choosing how many low-lying orbitals will be frozen during the CI calculations, and (b) how many virtual orbitals will be included in the CI calculations. In Fig. 2, we examine the convergence of the computed optical absorption spectrum of the three isomers of B₁₂, with respect to the choice of the active orbitals. Assuming that N_f implies the total number of frozen orbitals in the calculations, we performed three sets of calculations for each isomer: (i) $N_f = 12$, $N = 40/41/42$, (ii) $N_f = 12$, $N = 46$, and (iii) $N_f = 18$, $N = 40/41/42$. Here $N_f = 12$ implies that 1s core orbital of each boron atom of the cluster was frozen during the CI calculations, while for $N_f = 18$ implies that in addition to the atomic core orbitals, six additional orbitals were frozen during the calculations. Furthermore, for $N_f = 12$, total number of valence electrons considered in the CI calculations was $N_{val} = 36$, while for $N_f = 18$, this reduces to $N_{val} = 24$. When we examine the computed spectra, it is obvious that: (a) for the quasi-planar and the chain structures, three sets of calculations are in good qualitative and quantitative agreement with each other, (b) for the case of the double ring structure, three sets of calculations are in good agreement with each other for photon energy $E < 5$ eV, but at $E \approx 7$ eV, results of three sets of calculations differ from each other. Nevertheless, for the double ring, even in that energy region $N_f = 12$, $N = 42$ and $N_f = 12$, $N = 46$ calculations agree with each other as far as peak locations are concerned, but disagree on peak intensities. Therefore, we conclude that the calculations corresponding to $N_f = 12$, $N = 46$, are well converged, and analyze those results in the next section.

2.4. Size of the CI expansion.

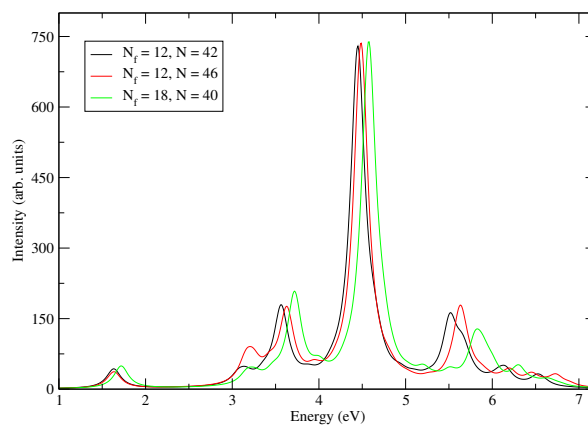
As mentioned previously, the MRSDCI procedure adopted in these calculations is iterative in nature. Thus, once the number of active/frozen orbitals N/N_f is fixed, MRSDCI procedure is iterated until the absorption spectrum converges within reasonable tolerance levels. In Table 2, we present the data regarding the final MRSDCI calculations performed on the three isomers, which includes: (a) point group symmetry used in the calculations, and (b) total number of configurations N_{total} in the MRSDCI expansion for various irreducible representations. We note that N_{total} ranges



(a) quasi-planar



(b) Double ring



(c) Chain

Figure 2: Optical absorption spectra of three most stable isomers of B_{12} , calculated using varying numbers of frozen and active orbitals.

Table 2: The average number of total configurations involved in MRSDCI calculations (N_{total}) of the optical absorption spectra of the most stable isomers of B_{12} cluster.

Isomer	Point group	Symmetry	N_{total}
Quasi-planar †	C_{3v}	A'	6903907
		A''	6207478
Double ring†	D_{6d}	A'	5210210
		A''	6741895
Chain	C_{2h}	A_g	556980
		A_u	9353654
		B_u	9588626

† C_s point group symmetry was used during the calculations

roughly from five millions to ten millions, implying that these were large-scale calculations, and, therefore, electron-correlation effects have been included to a high-level both for the ground state, and the excited states.

3. Results and Discussion

Next, we discuss the geometry and the electronic structure of isomers of B_{12} considered in this work. Furthermore, we also discuss the optical absorption spectra of three of the most stable isomers.

3.1. Icosahedron

This is one of the most studied isomers of the B_{12} cluster, perhaps, because of its high-level of symmetry, i.e., a perfect icosahedral structure, and I_h symmetry group.[24, 25, 8] Bambakidis and Wagner used the Slater’s SCF-Xa-SW approach to study the electronic structure and cohesive properties of B_{12} icosahedral cluster, while Boustani employed first-principles DFT and Hartree-Fock approaches to study it.[25, 8] Furthermore, B_{12} icosahedron forms the fundamental units in bulk boron, and other boron-rich solids, therefore, it has always made one curious whether or not it exists in isolated form.[6, 26, 27] Hayami[28] studied the encapsulation properties of the B_{12} icosahedral cluster using first-principles DFT based methodology. Kawai and Weare[6] based upon ab initio molecular dynamics simulations, and Boustani using first-principles DFT and Hartree-Fock methods,[25, 8] concluded that the isolated B_{12} icosahedral cluster is unstable, and actually stabilizes to a lower-energy open structure.

In order to examine the fundamental reasons behind the instability of the singlet I_h structure against structural distortions, we consider the possibility of Jahn-Teller effect, and to that end we examine the single-particle energy levels of B_{12} perfect icosahedron, obtained from calculations without any electrons. These calculations were performed using a STO-3G basis set, and the energy levels obtained, along with their symmetries, are shown in Fig. 3. If we start filling the energy levels using auf-bau principle, we note that the five-fold degenerate highest-occupied molecular orbital (HOMO) of H_g symmetry is partially filled, thus making the isomer a candidate for Jahn-Teller distortion to a structure of lower symmetry.

Another manifestation of this instability is that automated geometry optimization procedures, such as the one based on Berny algorithm implemented in Gaussian 09 package,[22] inevitably lead

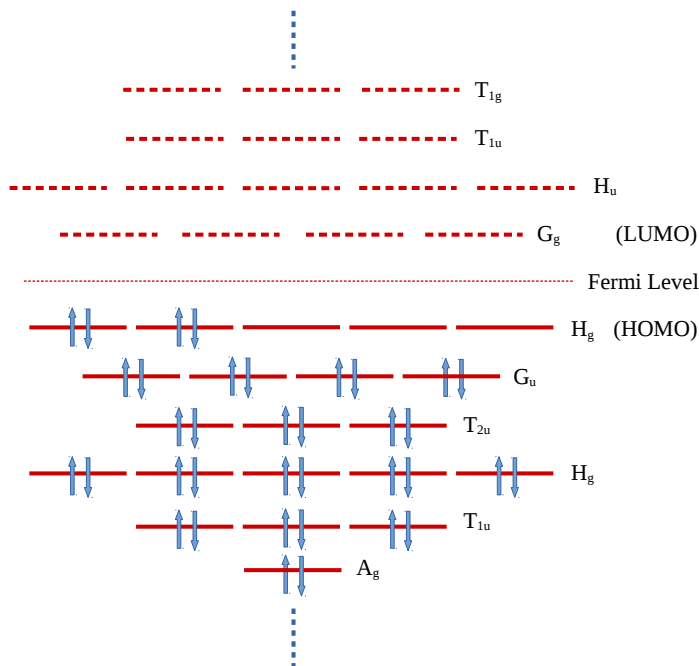


Figure 3: A rough sketch of orbital energies of B_{12} - icosahedron (I_h symmetry group), close to the Fermi level. Irreducible representations of the corresponding orbitals are indicated next to them. HOMO, with its five-fold degeneracy, is partially occupied, thereby making the system a candidate for Jahn-Teller distortion, to a lower symmetry structure.

to a lower symmetry structure, if the starting geometry is a perfect icosahedron, with I_h symmetry. Since we are interested in computing the total energy of the perfect icosahedral structure, we optimized corresponding geometry manually, by varying the nearest-neighbor bond length, and looking for the minimum of energies computed using the CCSD approach, and cc-PVDZ basis functions. At this point, an objection can be raised against the use of single-reference approaches such as CCSD to describe the ground state of the I_h structure, given the orbital degeneracy at the Fermi level as depicted in Fig. 3. However, this is not a problem if one uses the Hartree-Fock (HF) molecular orbitals (MOs) for performing the correlated-electron calculations, because the electron-electron repulsion lifts the orbital degeneracies to a great extent. Furthermore, we verified this by performing MRSDCI calculations on the I_h structure at its minimum energy geometry using the HF MOs, and found that the coefficient of the HF reference state is 0.81 in the lowest singlet-state wave function (see Table S16 of Supporting Information, and the related discussion), thereby, justifying the use of single-reference approaches to compute the ground state energy. The minimum energy I_h structure obtained from these CCSD/cc-PVDZ calculations is depicted in Fig. 1(e), with the corresponding total energy listed in Table 1. Next, we checked the stability of the perfect icosahedral structure by performing vibrational frequency analysis at the CCSD level, using the cc-PVDZ basis set, and found it to be unstable with five imaginary frequencies.

Next, we performed automated geometry optimization[22] on the icosahedral structure, with the starting atomic coordinates corresponding to the I_h structure, and 1.73 Å bond length corresponding to Fig. 1(e). The resultant optimized geometry has a distorted icosahedral structure with D_{2h} symmetry, with non-uniform nearest-neighbor distances in the range 1.71 Å—1.80 Å, as shown in Fig. 1(f). This distorted structure has an energy 3.55 eV higher than the quasi-planar structure, but 0.31 eV more stable as compared to the I_h structure. To explore the stability of this structure, we performed vibrational frequency analysis on it at the CCSD level, using the same cc-pVDZ basis

set, and found that it is a transition state, with one imaginary frequency. This, clearly reveals that perfect I_h structure of B_{12} cluster with the singlet spin is totally unstable, and deforms into a distorted icosahedral transition state corresponding to a saddle point on the potential energy surface. This indicates that this D_{2h} structure is itself unstable, and will undergo further distortions to achieve stability. Thus, our calculations have confirmed the instability of the I_h structure of the B_{12} cluster.

3.2. Quasi-planar convex structure

This lowest lying quasi-planar convex shaped isomer of B_{12} has C_{3v} point group symmetry, with the irreducible representation 1A_1 of the electronic ground state wave function. Several authors have theoretically studied this isomer earlier,[29, 30, 31] including one of us.[25, 8] Our geometry optimization study reveals this to be the most stable one amongst the eleven isomers studied (see Table 1), a result in good agreement with several earlier studies performed using lower levels of theory.[6, 25, 8] The optimized geometry of this isomer is shown in Fig. 1(a). This structure is composed of one outer ring with nine boron atoms, and an inner triangular ring with three boron atoms. The inner ring is slightly out of plane compared with the outer ring, and has larger bond length (1.71 Å) as compared to those in the outer ring (1.65 Å and 1.59 Å). Each inner boron atom is surrounded by six other boron atoms, thus this quasi-planar isomer consists of three dovetailed hexagonal pyramids. The reported bond lengths optimized using Hartree-Fock level of theory by one of us earlier are in good agreement with our present work.[8] The bond lengths obtained by us are in good agreement with those reported by Atis *et al.*[30] Existence of this isomer was verified experimentally by Wang *et al.*[29] and recently the unusual stability of this isomer was explained theoretically by Kiran and co-workers.[31] To understand the stability of this isomer from the Jahn-Teller perspective, we present the orbital occupancy diagram in Fig. 4 based upon a single-point Hartree-Fock calculation performed at the optimized geometry, using a cc-pVTZ basis set. From the figure it is obvious that even though the HOMO is two-fold degenerate, it is completely filled, and, therefore, as per Jahn-Teller theorem, it will not undergo any further distortion. To confirm this, we performed vibrational frequency analysis for this structure at the CCSD level theory using cc-pVDZ basis, and found it to be completely stable, with all the vibrational frequencies being real. The fact that this structure has the lowest-energy of all the isomers considered, also suggests that it is stable.

Because this is a stable isomer, we also calculated its ground state linear optical absorption spectra presented in Fig. 5. During the electron-correlated MRSDCI calculations, C_s point group symmetry was utilized. HOMO orbitals of this isomer are doubly degenerate, denoted as H_1 and H_2 , both of which are doubly occupied. From Fig. 5, it is obvious that absorption in this isomer starts with a very small peak (I) at 3.58 eV, followed by three weak peaks at 4.43 eV (II), 4.93 eV (III) and 5.44 eV (IV), which is a shoulder to the most intense peak (V) located at 5.74 eV. The wave function of the excited state corresponding to this peak is dominated by single excitation $(H - 3)_2 \rightarrow L_2$ and $(H - 3)_1 \rightarrow L_1$, with respect to the closed-shell Hartree-Fock reference configuration. Detailed information about the excited states contributing to the peaks, is presented in Table S1 of the supporting information.

3.3. Double ring

This structure is composed of two regular hexagons of B atoms, displaced from each other, without the boron atoms eclipsing each other, as shown in Fig. 1(b). As a result, this isomer has the D_{6d} point-group symmetry, along with a closed-shell 1A_1 electronic ground state, with its total energy 1.86 eV higher as compared to the lowest energy quasi-planar isomer. The bond length of two closest in-plane and out of plane boron atoms are 1.6458 Å and 1.7349 Å, in good agreement with recent work of Atis *et al.* [30] The top view of this isomer, with its two hexagonal rings visible, is presented in Fig. 6. Based upon the vibrational frequency analysis of this structure, we conclude that this

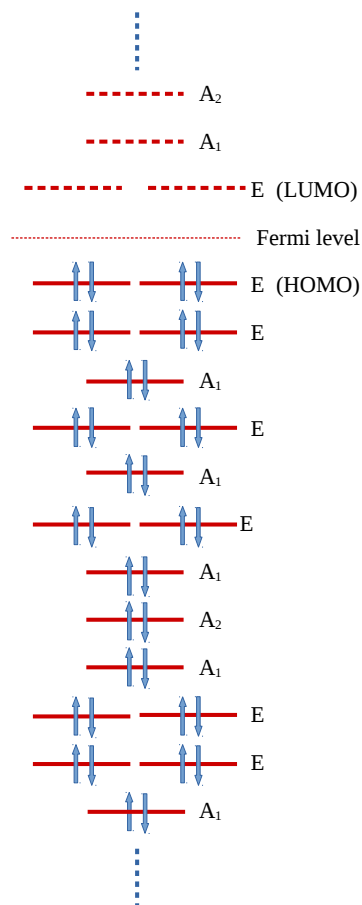


Figure 4: A rough sketch of the energy levels of quasi-planar (C_{3v}) isomer, along with a few low-lying virtual levels, obtained from the Hartree-Fock calculations performed at the optimized geometry, using a cc-pVTZ basis set. Irreducible representations of the orbitals corresponding to these levels, are indicated next to them. It is obvious that the doubly-degenerate HOMO is fully occupied for this isomer, indicating that it is stable against a Jahn-Teller distortion.

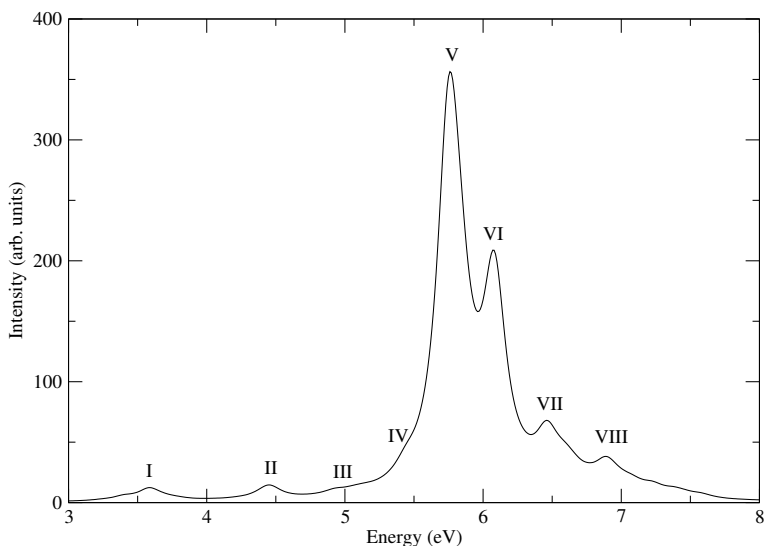


Figure 5: Linear optical absorption spectrum of quasi-planar isomer computed using the MRSDCI approach, and the cc-pVDZ basis set. During the calculations forty six active orbitals were used, while all the twelve 1s core orbitals were assumed frozen. To plot the spectrum, 0.1 eV uniform line-width was used.

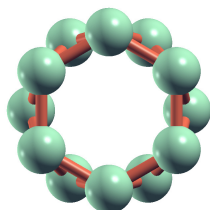


Figure 6: Double ring structure of B_{12} isomer (Top view).

isomer is stable, and as a result we have computed its optical absorption spectrum using the MRSDCI approach, presented in Fig. 7.

For the MRSDCI calculations C_s (Abelian) point group symmetry was employed, and in the Hartree-Fock ground state, doubly degenerate HOMO orbitals denoted as H_1 and H_2 were fully occupied. Other degenerate occupied and virtual molecular orbitals were also denoted by suffixes 1 and 2 etc. The detailed information about the wave functions of the excited states contributing to various peaks, along with the frontier orbitals involved in those excitations, are presented in Table S2, and Fig. 2, respectively, of the supporting information. The computed spectrum starts with a very intense peak (I), which is due to two nearly degenerate excited states around 4.8 eV, with wave functions dominated by singly-excited configurations $|(H - 1)_2 \rightarrow (L+1)_2\rangle$, $|(H - 1)_1 \rightarrow (L+1)_1\rangle$, $|(H - 1)_1 \rightarrow (L+1)_2\rangle$, and $|(H - 1)_2 \rightarrow (L+1)_1\rangle$. It is followed by two comparatively less intense peaks around 5.9 eV (II) and 6.4 eV (III), whose wave functions also consist mainly of the single excitations. The peak IV is the most intense peak near 6.8 eV, which is due to two nearly degenerate excited states, largely due to singly-excited electrons. We note that the absorption spectrum of this structure is sufficiently different, both qualitatively, and quantitatively, as compared to that of the quasi-planar isomer.

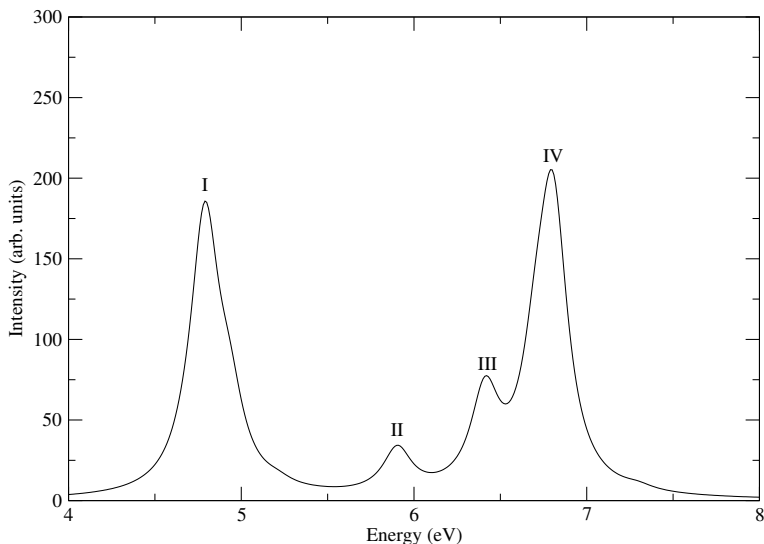


Figure 7: Linear optical absorption spectrum of B_{12} isomer with the double ring structure, calculated using the MRSDCI approach, and the cc-pVDZ basis set. During the calculations forty six active orbitals were used, while all the twelve 1s core orbitals were assumed frozen. To plot the spectrum, 0.1 eV uniform line-width is used.

3.4. Chain

Chain-like isomer of B_{12} is 2.86 eV higher in energy as compared to the lowest-energy quasi-planar structure, and has the structure of a ladder with rungs of the ladder not being parallel to each other (see Fig. 1(c)), with bond lengths ranging from 1.55 Å to 1.87 Å. The point group symmetry of the isomer is C_{2h} , with the electronic ground state symmetry 1A_g . We also performed the vibrational frequency analysis on this isomer, revealing it to be stable. As a result, we have calculated the optical absorption spectrum of this structure using the MRSDCI approach, and the results are presented in Figs. 8 and 9. In Fig. 8, we have plotted the component corresponding to the photons polarized in the plane of the chain, leading to the absorption to the 1B_u type excited states, and this component carries the bulk of the absorption intensity. In Fig. 9, we plot the absorption spectrum of the photons polarized perpendicular to the plane of the chain, corresponding to 1A_u excited states. We have plotted two absorption components separately because of the huge difference in the intensities involved. It is quite understandable that the bulk of the oscillator strength is carried by absorption polarized in the plane of the chain, because that is where the atoms, and hence, electrons are, leading to large transition dipole moments with respect to the ground state.

The in-plane absorption begins with a small peak (I) at 1.64 eV dominated by $|H \rightarrow L\rangle$ and $|H-1 \rightarrow L+1\rangle$. The most intense peak (V) appears near about 4.5 eV dominated by $|H \rightarrow L\rangle$ and $|H-1 \rightarrow L+1\rangle$ single excitations. From Fig. 3 of supporting information it is obvious that the orbitals involved $H-1/L+1$ have π/π^* character, while H/L have σ/σ^* character, thus these transition have a mixed $\pi - \pi^* + \sigma - \sigma^*$ character. The detailed many-particle wave functions of the excited states associated with the peaks of the optical absorption spectra are presented in Table S3 of the supporting information.

As far as the out-of-plane component of the absorption spectrum is concerned, it is obvious from Fig. 9 and from Table S4 of the supporting information, that oscillator strengths corresponding to peaks are at least two orders of magnitude smaller than those of “in-plane” component. This component of the absorption starts at 2.42 eV, with its most intense peak IV located at 4.85 eV. From Table S4, it is clear that the wave functions of the excited states contributing to the peaks are dominated by singly excited configurations involving orbitals away from the Fermi level, and doubly excited configurations involving orbitals close to the Fermi level. However, detection of these

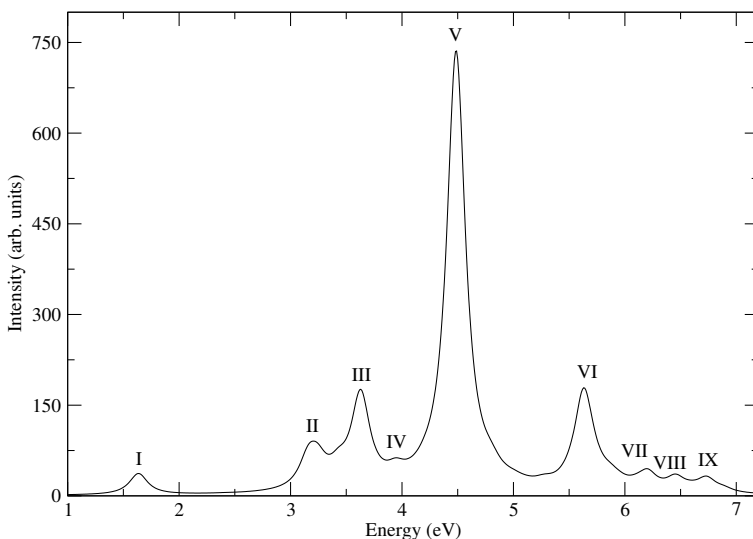


Figure 8: Linear optical absorption spectrum of chain-like B_{12} isomer using the MRSDCI approach, and the cc-pVDZ basis set, for the photons polarized in the plane of the chain, *i.e.*, for excited states of 1B_u symmetry. During the calculations forty six active orbitals were used, while all the twelve 1s core orbitals were assumed frozen. To plot the spectrum, 0.1 eV uniform line-width is considered.

resonances will be a difficult task unless it is possible to orient the isomer perpendicular to the polarization direction of the incident photons.

Comparison of the optical absorption spectrum of the chain isomer with those of the quasi-planar and the double ring structures, clearly reveals qualitative and quantitative differences which can be utilized as the fingerprints of these structures, and thus can be used in their optical detection.

3.5. Hexagons

This planar isomer belongs to D_{2h} point group with the electronic ground state symmetry 1A_g and has the appearance of a boron dimer surrounded by ten other boron atoms. One of us discovered this structure earlier using Hartree-Fock level geometry optimization, and a 3-21G basis set.[8] In this work the optimized geometry obtained using the CCSD level of theory, and cc-pVDZ basis set, is shown in Fig. 1(d). For this structure, the average bond length in between two consecutive peripheral boron atoms is 1.56 Å, while the bond length between any of the central atom, and the closest peripheral atom is near about 1.8 Å.

3.6. Quad

This isomer has a three-dimensional structure shown in Fig. 1(g), with a D_{2h} point group, along with the electronic ground state of symmetry 1A_g . The structure consists of two six-membered rings of boron atoms, lying in mutually perpendicular planes. In one plane the B-B bond lengths are almost equal, *i.e.*, near about 1.65 Å, but in the other plane it has two distinct bond lengths of 1.72 Å and 1.83 Å. This isomer is predicted to be 5.17 eV higher in energy as compared to the lowest energy one.

3.7. Pris-3-square-1

This isomer also has a three-dimensional structure of a cuboidal shape, whose two faces are squares, while the remaining four are rectangles. The length of the sides of square shaped faces is 1.73 Å, and the two squares are 2.53 Å apart from each other. Furthermore, four opposite faces as shown in Fig. 1(h) are capped by a boron atom each in a symmetric manner, with the nearest

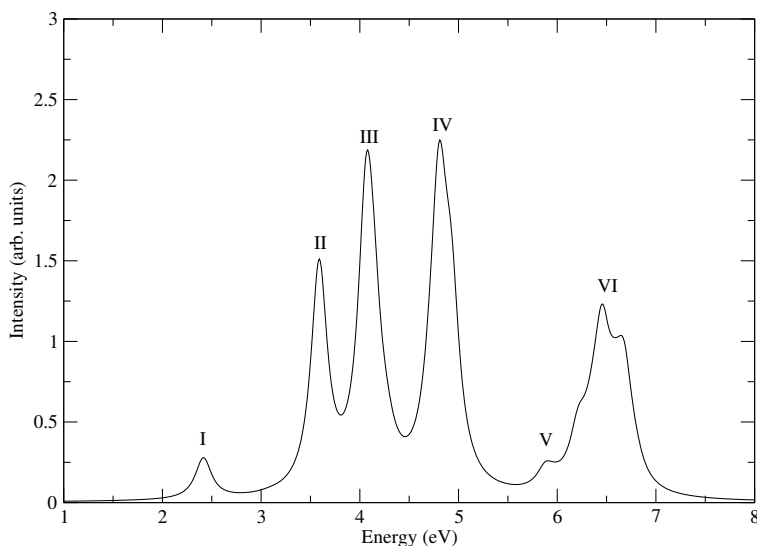


Figure 9: Linear optical absorption spectrum of chain-like B_{12} isomer, corresponding to the excited states of A_u symmetry, with the photons polarized perpendicular to plane of the chain. Spectrum was computed using the MRSDCI approach, and the cc-pVDZ basis set. During the calculations forty six active orbitals were used, while all the twelve $1s$ core orbitals were assumed frozen. To plot the spectrum, 0.1 eV uniform line-width is considered.

distance between the capping atom and the cube atom being 1.69 Å. This structure has D_{4h} point group symmetry, and it is 8.5 eV higher in energy than the lowest energy one, with the electronic ground state symmetry $^1A_{1g}$.

3.8. *Pris-3-square-2*

This isomer has a very similar structure as Pris-3-square isomer discussed in the previous section, except that the length of the sides of the square-shaped faces is slightly larger at 1.79 Å, and the distance between the opposite squares is slightly shorter at 1.98 Å. As shown in Fig. 1(i), distance of the capping atoms from the corresponding faces is also slightly shorter at 1.66 Å. With a structure similar to that Pris-3-square-1, this isomer also has D_{4h} point group symmetry, with the electronic ground state symmetry of $^1A_{1g}$. In spite of a structure similar to that of Pris-3-square-1 isomer, it is energetically about 2 eV higher than that, and 10.58 eV higher than the lowest energy quasi-planar structure.

3.9. *Parallel triangular*

B_{12} - parallel triangular isomer has D_{3h} point group symmetry, with the electronic ground state symmetry $^1A'_1$. As shown in Fig. 1(j), it consists of four parallel equilateral triangles arranged symmetrically about a central plane. The first/last of those triangles has edge length 1.71 Å, while the two middle triangles have equal bond lengths of 1.85 Å. The connecting bond length in between two middle triangles have edge length 1.85 Å. The interplanar distances between the first two and the last two triangles is close to 1.6 Å, while that between the middle triangles is 1.85 Å. This structure is roughly 12 eV higher in energy as compared to the lowest energy structure.

3.10. *Planar square*

This isomer which is about 13.5 eV higher than the lowest energy structure, is strictly a planar one, with the D_{4h} point group, and the electronic ground state symmetry $^1A_{1g}$. As shown in Fig. 1(k), it is composed of four isosceles trapezoids connecting with each other at a common side, resulting in a square-like symmetry. The equal sides of isosceles trapezoid have the bond length of 1.75 Å, while the other two sides have the bond lengths of 1.56 Å, and 1.66 Å.

4. Conclusions

In conclusion, we presented a detailed *ab initio* electron-correlated study of the electronic structure and the ground state geometries of several isomers of B₁₂ cluster. In agreement with the earlier works, quasi-planar convex structure was found to be the lowest energy structures, however, several other structures corresponding to the local minima on the potential energy surface were also identified. In particular, our calculations confirm that B₁₂ perfect icosahedral structure with I_h symmetry is unstable against structural distortions. Furthermore, Jahn-Teller analysis of the icosahedral isomer revealed that it may be unstable because at the single-electron level of theory, it has several unfilled degenerate HOMO orbitals. On the other hand, a similar analysis of the lowest-energy quasi-planar structure reveals that the isomer has completely filled doubly-degenerate HOMO, signaling its stability against Jahn-Teller distortion. These results are also in agreement with the vibrational frequency analysis which also predicts the singlet I_h structure to be unstable, and the quasi-planar structure to be stable. However, whether Jahn-Teller distortion causes B₁₂ perfect icosahedron into the quasi-planar structure, can be resolved by other calculations, such as the ones based upon linear-transit theory connecting the potential energy surface of the I_h structure, to that of the quasi-planar one, which at present is beyond the scope of this work. Vibrational frequency analysis also predicted two other isomers, namely double ring, and the chain structures, to be stable. For these three stable structures, namely, quasi-planar, double ring, and the chain isomer, we also calculated the optical absorption spectra employing the state-of-the-art MRSDCI methodology, utilizing large-scale CI expansions. The calculated spectra revealed strong structure-property relationship which can be utilized for detection of different isomers using optical techniques.

Acknowledgements

Work of P.B. was supported by a Senior Research Fellowship offered by University Grants Commission, India.

References

- [1] Walt A. de Heer. The physics of simple metal clusters: experimental aspects and simple models. *Rev. Mod. Phys.*, 65:611–676, Jul 1993.
- [2] Zheng Li, Zheng Liu, Haiyan Sun, and Chao Gao. Superstructured assembly of nanocarbons: Fullerenes, nanotubes, and graphene. *Chemical Reviews*, 115(15):7046–7117, 2015. PMID: 26168245.
- [3] Ihsan Boustani. Towards novel boron nanostructural materials. 8:1–44, 2011.
- [4] Andrew J. Mannix, Brian Kiraly, Mark C. Hersam, and Nathan P. Guisinger. Synthesis and chemistry of elemental 2d materials. *Nature Reviews Chemistry*, 1:0014, 2017.
- [5] Luke Hanley, Jerry L. Whitten, and Scott L. Anderson. Collision-induced dissociation and *ab initio* studies of boron cluster ions: determination of structures and stabilities. *The Journal of Physical Chemistry*, 92(20):5803–5812, 1988.
- [6] R. Kawai and J. H. Weare. Instability of the b12 icosahedral cluster: Rearrangement to a lower energy structure. *The Journal of Chemical Physics*, 95(2):1151–1159, 1991.
- [7] Hiroshi Kato and Eishi Tanaka. Stabilities of small ben and bn clusters (n = 4-8) by vibrational analysis. *Journal of Computational Chemistry*, 12(9):1097–1109, 1991.

- [8] Ihsan Boustani. Systematic ab initio investigation of bare boron clusters: determination of the geometry and electronic structures of B_n ($n=2-14$). *Phys. Rev. B*, 55:16426–16438, Jun 1997.
- [9] Albert B. and Hillebrecht H. Boron: elementary challenge for experimenters and theoreticians. *Angew. Chem. Int. Ed. Engl.*, 48:8640–68, 2009.
- [10] A. R. Oganov, J. H. Chen, C. Gatti, Y. Z. Ma, Y. M. Ma, C. W. Glass, Z. X. Liu, T. Yu, O. O. Kurakevych, and V. L. Solozhenko. Ionic high-pressure form of elemental boron. *Nature*, 457:863–867, 2009.
- [11] Alok Shukla. Correlated theory of triplet photoinduced absorption in phenylene-vinylene chains. *Phys. Rev. B*, 65:125204, Mar 2002.
- [12] Alok Shukla. Theory of nonlinear optical properties of phenyl-substituted polyacetylenes. *Phys. Rev. B*, 69:165218, Apr 2004.
- [13] Priya Sony and Alok Shukla. Large-scale correlated calculations of linear optical absorption and low-lying excited states of polyacenes: Pariser-parr-pople hamiltonian. *Phys. Rev. B*, 75:155208, Apr 2007.
- [14] Himanshu Chakraborty and Alok Shukla. Pariser-parr-pople model based investigation of ground and low-lying excited states of long acenes. *The Journal of Physical Chemistry A*, 117(51):14220–14229, 2013.
- [15] Himanshu Chakraborty and Alok Shukla. Theory of triplet optical absorption in oligoacenes: From naphthalene to heptacene. *The Journal of Chemical Physics*, 141(16):–, 2014.
- [16] Karan Aryanpour, Alok Shukla, and Sumit Mazumdar. Electron correlations and two-photon states in polycyclic aromatic hydrocarbon molecules: A peculiar role of geometry. *The Journal of Chemical Physics*, 140(10):–, 2014.
- [17] Tista Basak, Himanshu Chakraborty, and Alok Shukla. Theory of linear optical absorption in diamond-shaped graphene quantum dots. *Phys. Rev. B*, 92:205404, Nov 2015.
- [18] Shinde Ravindra and Shukla Alok. Large-scale first principles configuration interaction calculations of optical absorption in boron clusters. *Nano LIFE*, 02(02):1240004, 2012.
- [19] Shinde Ravindra and Shukla Alok. Large-scale first principles configuration interaction calculations of optical absorption in aluminum clusters. *Phys. Chem. Chem. Phys.*, 16:20714–20723, 2014.
- [20] Pradip Kumar Priya, Deepak Kumar Rai, and Alok Shukla. Photoabsorption in sodium clusters: first principles configuration interaction calculations. *Eur. Phys. J. D*, 71:116, 2017.
- [21] Ravindra Shinde and Alok Shukla. First principles electron-correlated calculations of optical absorption in magnesium clusters. *Eur. Phys. J. D*, 71:301, 2017.
- [22] M. J. Frisch, G. W. Trucks, H. B. Schlegel, G. E. Scuseria, M. A. Robb, J. R. Cheeseman, G. Scalmani, V. Barone, B. Mennucci, G. A. Petersson, H. Nakatsuji, M. Caricato, X. Li, H. P. Hratchian, A. F. Izmaylov, J. Bloino, G. Zheng, J. L. Sonnenberg, M. Hada, M. Ehara, K. Toyota, R. Fukuda, J. Hasegawa, M. Ishida, T. Nakajima, Y. Honda, O. Kitao, H. Nakai, T. Vreven, J. A. Montgomery, Jr., J. E. Peralta, F. Ogliaro, M. Bearpark, J. J. Heyd, E. Brothers, K. N. Kudin, V. N. Staroverov, R. Kobayashi, J. Normand, K. Raghavachari, A. Rendell, J. C.

- Burant, S. S. Iyengar, J. Tomasi, M. Cossi, N. Rega, J. M. Millam, M. Klene, J. E. Knox, J. B. Cross, V. Bakken, C. Adamo, J. Jaramillo, R. Gomperts, R. E. Stratmann, O. Yazyev, A. J. Austin, R. Cammi, C. Pomelli, J. W. Ochterski, R. L. Martin, K. Morokuma, V. G. Zakrzewski, G. A. Voth, P. Salvador, J. J. Dannenberg, S. Dapprich, A. D. Daniels, O. Farkas, J. B. Foresman, J. V. Ortiz, J. Cioslowski, and D. J. Fox. Gaussian 09 Revision E.01. Gaussian Inc. Wallingford CT 2009.
- [23] L. E. McMurchie, S. T. Elbert, S. R. Langhoff, and E. R. Davidson. MELD package from Indiana University. It has been modified by us to handle bigger systems.
- [24] G. Bambakidis and R. P. Wagner. Electronic structure and binding energy of the icosahedral boron cluster b_{12} . *Journal of Phys. Chem. Solids*, 42:1023–1025, 1981.
- [25] Ihsan Boustani. Structure and stability of small boron clusters. a density functional theoretical study. *Chemical Physics Letters*, 240(1):135 – 140, 1995.
- [26] Hervé Hubert, Bertrand Devouard, Laurence A. J. Garvie, Michael O’Keeffe, Peter R. Buseck, William T. Petuskey, and Paul F. McMillan. Icosahedral packing of b_{12} icosahedra in boron suboxide (b_{60}). *Nature*, 391:376 – 378, 1998.
- [27] Craig L. Perkins, Michael Trenary, and Takaho Tanaka. Direct observation of (B_{12}) $(B_{12})_{12}$ supericosahedra as the basic structural element in yb_{66} . *Phys. Rev. Lett.*, 77:4772–4775, Dec 1996.
- [28] Wataru Hayami. Theoretical study of the stability of ab_{12} ($a = H - Ne$) icosahedral clusters. *Phys. Rev. B*, 60:1523–1526, Jul 1999.
- [29] H. J. Zhai, B. Kiran, J. Li, and L. S. Wang. Hydrocarbon analogues of boron clusters - planarity, aromaticity and antiaromaticity. *Nature Materials*, 2:827 – 833, 2003.
- [30] Murat Atis, Cem Ozdogan, and Ziya B. Guvenc. Structure and energetic of bn ($n = 2-12$) clusters: Electronic structure calculations. *International Journal of Quantum Chemistry*, 107(3):729–744, 2007.
- [31] Boggavarapu Kiran, G. Gopa Kumar, Minh T. Nguyen, Anil K. Kandalam, and Puru Jena. Origin of the unusual stability of b_{12} and b_{13+} clusters. *Inorganic Chemistry*, 48(21):9965–9967, 2009. PMID: 19785465.

Supporting Information: First Principles Study of Structural and Optical Properties of B₁₂ Isomers

Pritam Bhattacharyya

Department of Physics, Indian Institute of Technology Bombay, Powai, Mumbai 400076, India

Ihsan Boustani

Theoretical and Physical Chemistry, Faculty of Mathematics and Natural Sciences, Bergische Universität, Wuppertal, Gauss Strasse 20, D-42097 Wuppertal, Germany

Alok Shukla

Department of Physics, Indian Institute of Technology Bombay, Powai, Mumbai 400076, India

Here we present the plots of the frontier orbitals, and the wave functions of important excited states contributing to the calculated optical absorption spectra of three B₁₂ isomers, namely: (a) quasi-planar, (b) double ring, and (c) chain.

1. Quasi-Planar Isomer

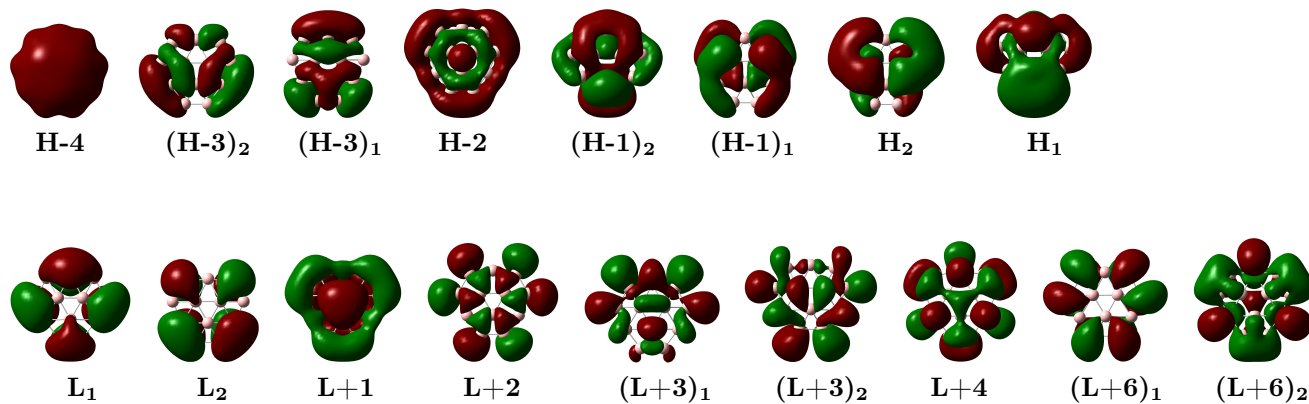
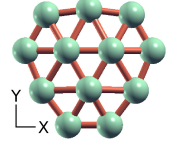


Figure 1: Frontier molecular orbitals of quasi-planar (C_{3v}) isomer of B₁₂ (see Fig. 1a, of the main article), contributing to important peaks in its optical absorption spectra. The symbols H and L corresponds to HOMO and LUMO orbitals. Subscripts 1, 2 etc. are used to label the degenerate orbitals.

Email addresses: pritambhattacharyya01@gmail.com (Pritam Bhattacharyya), boustani@uni-wuppertal.de (Ihsan Boustani), shukla@phy.iitb.ac.in (Alok Shukla)

Table S1: Many-particle wave functions of the excited states associated with the peaks in the optical absorption spectra of quasi-planar (C_{3v}) isomer of B_{12} (Fig. 1a of the main article). E denotes the excitation energy (in eV) of the state involved, and f stands for oscillator strength corresponding to the electric-dipole transition to that state, from the ground state. In the ‘‘Polarization’’ column, x, y, and z denote the the direction of polarization of the absorbed light, with respect to the Cartesian coordinate axes defined in the figure below. In the ‘‘Wave function’’ column, $|HF\rangle$ indicates the Hartree-Fock (HF) configuration, while other configurations are defined as virtual excitations with respect to it. H and L denote HOMO and LUMO orbitals, while the degenerate orbitals are denoted by additional subscripts 1, 2 etc. In parentheses next to each configuration, its coefficient in the CI expansion is indicated. Below, GS does not indicate



a peak, rather it denotes the ground states wave function of the isomer.

Peak	E (eV)	f	Polarization	Wave function																																			
GS				$ HF\rangle(0.8882)$																																			
I	3.58	0.6317	y/z	$ H_2 \rightarrow L_2\rangle(0.4915)$ $ H_1 \rightarrow L_1\rangle(0.4898)$																																			
II	4.43	0.3851	y/z	$ (H-1)_1 \rightarrow L+1\rangle(0.4715)$ $ H_2 \rightarrow L+2\rangle(0.4434)$		4.46	0.3518	x	$ (H-1)_2 \rightarrow L+1\rangle(0.5284)$ $ H_1 \rightarrow L+2\rangle(0.4022)$	III	4.93	0.1464	y/z	$ (H-1)_2 \rightarrow L+2\rangle(0.6251)$ $ H_2 \rightarrow L+2\rangle(0.5838)$		5.07	0.1238	x	$ H-2 \rightarrow L_2\rangle(0.7529)$ $ H_1 \rightarrow L+2\rangle(0.3081)$	IV	5.44	0.7118	y/z	$ H-2 \rightarrow L+1\rangle(0.8518)$ $ H_1 \rightarrow L+1; H_2 \rightarrow L_2\rangle(0.0586)$	V	5.74	8.5755	x	$ (H-3)_1 \rightarrow L_2\rangle(0.6017)$ $ (H-1)_1 \rightarrow L+2\rangle(0.2998)$		5.76	11.1191	y/z	$ (H-3)_2 \rightarrow L_2\rangle(0.3757)$ $ (H-3)_1 \rightarrow L_1\rangle(0.3679)$		5.83	4.4994	x	$ (H-3)_2 \rightarrow L_1\rangle(0.5156)$ $ (H-3)_1 \rightarrow L_2\rangle(0.4430)$
	4.46	0.3518	x	$ (H-1)_2 \rightarrow L+1\rangle(0.5284)$ $ H_1 \rightarrow L+2\rangle(0.4022)$	III	4.93	0.1464	y/z	$ (H-1)_2 \rightarrow L+2\rangle(0.6251)$ $ H_2 \rightarrow L+2\rangle(0.5838)$		5.07	0.1238	x	$ H-2 \rightarrow L_2\rangle(0.7529)$ $ H_1 \rightarrow L+2\rangle(0.3081)$	IV	5.44	0.7118	y/z	$ H-2 \rightarrow L+1\rangle(0.8518)$ $ H_1 \rightarrow L+1; H_2 \rightarrow L_2\rangle(0.0586)$	V	5.74	8.5755	x	$ (H-3)_1 \rightarrow L_2\rangle(0.6017)$ $ (H-1)_1 \rightarrow L+2\rangle(0.2998)$		5.76	11.1191	y/z	$ (H-3)_2 \rightarrow L_2\rangle(0.3757)$ $ (H-3)_1 \rightarrow L_1\rangle(0.3679)$		5.83	4.4994	x	$ (H-3)_2 \rightarrow L_1\rangle(0.5156)$ $ (H-3)_1 \rightarrow L_2\rangle(0.4430)$					
III	4.93	0.1464	y/z	$ (H-1)_2 \rightarrow L+2\rangle(0.6251)$ $ H_2 \rightarrow L+2\rangle(0.5838)$		5.07	0.1238	x	$ H-2 \rightarrow L_2\rangle(0.7529)$ $ H_1 \rightarrow L+2\rangle(0.3081)$	IV	5.44	0.7118	y/z	$ H-2 \rightarrow L+1\rangle(0.8518)$ $ H_1 \rightarrow L+1; H_2 \rightarrow L_2\rangle(0.0586)$	V	5.74	8.5755	x	$ (H-3)_1 \rightarrow L_2\rangle(0.6017)$ $ (H-1)_1 \rightarrow L+2\rangle(0.2998)$		5.76	11.1191	y/z	$ (H-3)_2 \rightarrow L_2\rangle(0.3757)$ $ (H-3)_1 \rightarrow L_1\rangle(0.3679)$		5.83	4.4994	x	$ (H-3)_2 \rightarrow L_1\rangle(0.5156)$ $ (H-3)_1 \rightarrow L_2\rangle(0.4430)$										
	5.07	0.1238	x	$ H-2 \rightarrow L_2\rangle(0.7529)$ $ H_1 \rightarrow L+2\rangle(0.3081)$	IV	5.44	0.7118	y/z	$ H-2 \rightarrow L+1\rangle(0.8518)$ $ H_1 \rightarrow L+1; H_2 \rightarrow L_2\rangle(0.0586)$	V	5.74	8.5755	x	$ (H-3)_1 \rightarrow L_2\rangle(0.6017)$ $ (H-1)_1 \rightarrow L+2\rangle(0.2998)$		5.76	11.1191	y/z	$ (H-3)_2 \rightarrow L_2\rangle(0.3757)$ $ (H-3)_1 \rightarrow L_1\rangle(0.3679)$		5.83	4.4994	x	$ (H-3)_2 \rightarrow L_1\rangle(0.5156)$ $ (H-3)_1 \rightarrow L_2\rangle(0.4430)$															
IV	5.44	0.7118	y/z	$ H-2 \rightarrow L+1\rangle(0.8518)$ $ H_1 \rightarrow L+1; H_2 \rightarrow L_2\rangle(0.0586)$	V	5.74	8.5755	x	$ (H-3)_1 \rightarrow L_2\rangle(0.6017)$ $ (H-1)_1 \rightarrow L+2\rangle(0.2998)$		5.76	11.1191	y/z	$ (H-3)_2 \rightarrow L_2\rangle(0.3757)$ $ (H-3)_1 \rightarrow L_1\rangle(0.3679)$		5.83	4.4994	x	$ (H-3)_2 \rightarrow L_1\rangle(0.5156)$ $ (H-3)_1 \rightarrow L_2\rangle(0.4430)$																				
V	5.74	8.5755	x	$ (H-3)_1 \rightarrow L_2\rangle(0.6017)$ $ (H-1)_1 \rightarrow L+2\rangle(0.2998)$		5.76	11.1191	y/z	$ (H-3)_2 \rightarrow L_2\rangle(0.3757)$ $ (H-3)_1 \rightarrow L_1\rangle(0.3679)$		5.83	4.4994	x	$ (H-3)_2 \rightarrow L_1\rangle(0.5156)$ $ (H-3)_1 \rightarrow L_2\rangle(0.4430)$																									
	5.76	11.1191	y/z	$ (H-3)_2 \rightarrow L_2\rangle(0.3757)$ $ (H-3)_1 \rightarrow L_1\rangle(0.3679)$		5.83	4.4994	x	$ (H-3)_2 \rightarrow L_1\rangle(0.5156)$ $ (H-3)_1 \rightarrow L_2\rangle(0.4430)$																														
	5.83	4.4994	x	$ (H-3)_2 \rightarrow L_1\rangle(0.5156)$ $ (H-3)_1 \rightarrow L_2\rangle(0.4430)$																																			

(CONTINUED)

Table S1 – CONTINUES FROM THE PREVIOUS PAGE

Peak	E (eV)	f	Polarization	Wave function
VI	6.07	6.5321	y/z	$ (H-3)_2 \rightarrow L_2\rangle(0.4341)$
				$ (H-3)_1 \rightarrow L_1\rangle(0.4305)$
	6.09	4.6717	x	$ (H-3)_2 \rightarrow L_1\rangle(0.5747)$
				$ (H-3)_1 \rightarrow L_2\rangle(0.2940)$
VII	6.46	1.3019	y/z	$ H_1 \rightarrow (L+3)_1\rangle(0.5743)$
				$ H-4 \rightarrow L_1\rangle(0.3075)$
	6.46	1.1134	x	$ H-4 \rightarrow L_2\rangle(0.5028)$
				$ (H-3)_2 \rightarrow L+1\rangle(0.2557)$
	6.59	0.8096	x	$ H_1 \rightarrow (L+3)_2\rangle(0.5504)$
			$ H_2 \rightarrow (L+3)_1\rangle(0.3998)$	
VIII	6.88	0.9803	y/z	$ H_1 \rightarrow (L+6)_1\rangle(0.4043)$
				$ (H-1)_1 \rightarrow (L+3)_1\rangle(0.3240)$
	6.92	0.4733	x	$ H_2 \rightarrow (L+6)_1\rangle(0.3334)$
				$ H_2 \rightarrow L_1; H_2 \rightarrow L_2\rangle(0.3249)$

2. Double Ring Isomer

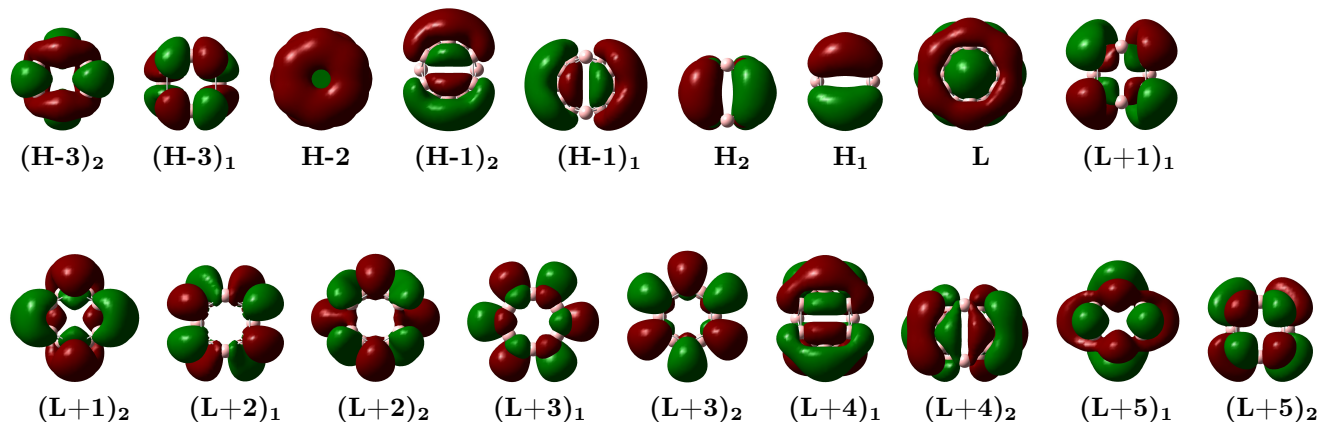
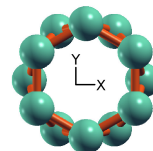


Figure 2: Frontier molecular orbitals of double ring (D_{6d}) isomer of B_{12} (see Fig. 1b, of the main article), contributing to important peaks in its optical absorption spectra. The symbols H and L corresponds to HOMO and LUMO orbitals. Subscripts 1,2 etc. are used to label the degenerate orbitals.

Table S2: Many particle wave functions of the excited states associated with the peaks in the optical absorption spectra of the double ring (D_{6d}) isomer of B_{12} (Fig. 1b, main article). E denotes the excitation energy (in eV) of the state involved, and f stands for oscillator strength corresponding to the electric-dipole transition to that state, from the ground state. In the ‘‘Polarization’’ column, x, y, and z denote the the direction of polarization of the absorbed light, with respect to the Cartesian coordinate axes defined in the figure below. In the ‘‘Wave function’’ column, $|HF\rangle$ indicates the Hartree-Fock (HF) configuration, while other configurations are defined as virtual excitations with respect to it. H and L denote HOMO and LUMO orbitals, while the degenerate orbitals are denoted by additional subscripts 1, 2 etc. In parentheses next to each configuration, its coefficient in the CI expansion is indicated. Below, GS does not indicate



a peak, rather it denotes the ground states wave function of the isomer.

Peak	E (eV)	f	Polarization	Wave function
GS				$ HF\rangle(0.8971)$
I	4.78	5.7331	y	$ (H-1)_2 \rightarrow (L+1)_2\rangle(0.5539)$ $ (H-1)_1 \rightarrow (L+1)_1\rangle(0.5442)$
	4.79	5.4136	x	$ (H-1)_1 \rightarrow (L+1)_2\rangle(0.5360)$ $ (H-1)_2 \rightarrow (L+1)_1\rangle(0.5224)$
	4.93	2.7899	z	$ H_2 \rightarrow (L+4)_2\rangle(0.6124)$ $ H-2 \rightarrow L\rangle(0.4341)$
II	5.90	1.8173	z	$ (H-1)_1 \rightarrow (L+4)_1\rangle(0.4577)$ $ (H-1)_2 \rightarrow (L+4)_2\rangle(0.4178)$
	III	6.41	3.9347	z
VI		6.80	6.1390	y
	6.81	5.3021	x	$ (H-3)_2 \rightarrow (L+3)_1\rangle(0.4368)$ $ H_1 \rightarrow (L+5)_2\rangle(0.3998)$

3. Chain Isomer

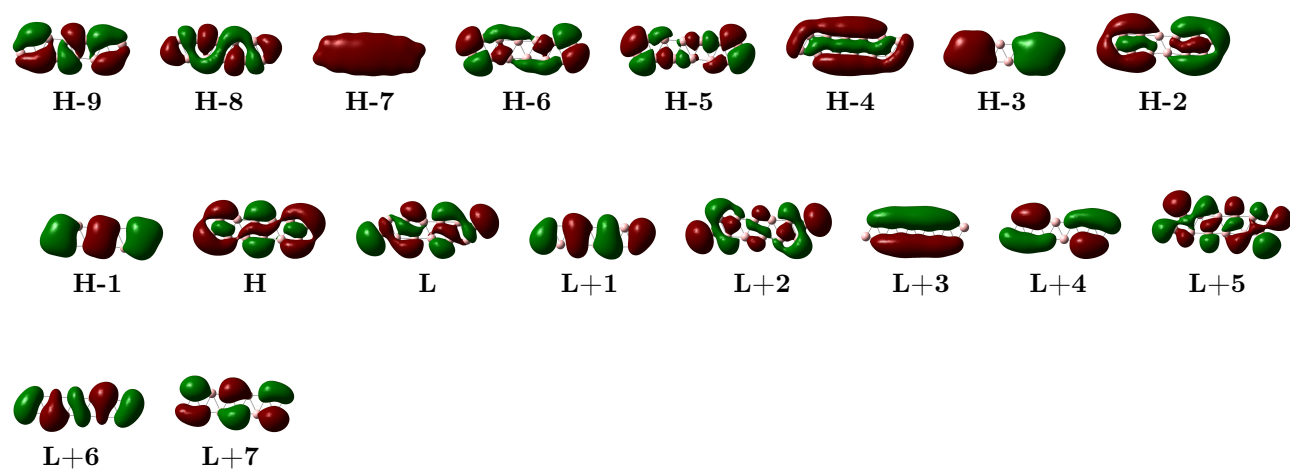


Figure 3: Frontier molecular orbitals of chain (C_{2h}) isomer of B_{12} (see Fig. 1c, of the main article), contributing to important peaks in its optical absorption spectra. The symbols H and L corresponds to HOMO and LUMO orbitals.

Table S3: Many-particle wave functions of the excited states associated with the peaks in the optical absorption spectrum of the chain (C_{2h}) isomer of B_{12} [Fig. 1c, main article], corresponding to excited states of B_u symmetry. E denotes the excitation energy (in eV) of the state involved, and f stands for oscillator strength corresponding to the electric-dipole transition to that state, from the ground state. In the ‘‘Polarization’’ column, x , y , and z denote the the direction of polarization of the absorbed light, with respect to the Cartesian coordinate axes defined in the figure below. In the ‘‘Wave function’’ column, $|HF\rangle$ indicates the Hartree-Fock (HF) configuration, while other configurations are defined as virtual excitations with respect to it. H and L denote HOMO and LUMO orbitals, while the degenerate orbitals are denoted by additional subscripts 1, 2 etc. In parentheses next to each configuration, its coefficient in the CI expansion is indicated. Below, GS does not indicate a peak, rather it denotes the ground states wave function of the isomer. All transitions correspond to photons polarized in plane of the chain.

Peak	E (eV)	f	Wave function
GS			$ HF\rangle(0.8367)$ $ H \rightarrow L; H \rightarrow L\rangle(0.2095)$
I	1.64	2.3438	$ H \rightarrow L\rangle(0.6916)$ $ H - 1 \rightarrow L + 1\rangle(0.3994)$
II	3.16	3.1597	$ H \rightarrow L + 5\rangle(0.3966)$ $ H - 1 \rightarrow L + 1\rangle(0.3600)$
	3.24	2.5110	$ H - 1 \rightarrow L + 3\rangle(0.6241)$ $ H - 7 \rightarrow L\rangle(0.3219)$
III	3.63	9.6596	$ H - 4 \rightarrow L\rangle(0.5134)$ $ H - 1 \rightarrow L + 1\rangle(0.3374)$
IV	3.94	1.2794	$ H - 5 \rightarrow L + 2\rangle(0.4566)$ $ H \rightarrow L; H - 5 \rightarrow L\rangle(0.3762)$
V	4.49	48.6542	$ H - 1 \rightarrow L + 1\rangle(0.4369)$ $ H \rightarrow L\rangle(0.3285)$
VI	5.63	10.3584	$ H - 8 \rightarrow L\rangle(0.5171)$ $ H - 6 \rightarrow L + 1\rangle(0.2364)$
VII	6.20	1.7806	$ H - 3 \rightarrow L + 4\rangle(0.3575)$ $ H \rightarrow L + 2; H - 1 \rightarrow L + 1\rangle(0.2426)$
VIII	6.46	1.3157	$ H - 6 \rightarrow L + 3\rangle(0.5479)$ $ H - 1 \rightarrow L + 7\rangle(0.2820)$
IX	6.74	0.8341	$ H - 9 \rightarrow L + 2\rangle(0.2964)$ $ H - 1 \rightarrow L + 7\rangle(0.2485)$

Table S4: Many-particle wave functions of the excited states corresponding to the peaks in the optical absorption spectrum of the chain (C_{2h}) isomer of B_{12} [Fig. 1c, main article], corresponding to excited states of A_u symmetry. E denotes the excitation energy (in eV) of the state involved, and f stands for oscillator strength corresponding to the electric-dipole transition to that state, from the ground state. In the “Polarization” column, x, y, and z denote the the direction of polarization of the absorbed light, with respect to the Cartesian coordinate axes defined in the figure below. In the “Wave function” column, $|HF\rangle$ indicates the Hartree-Fock (HF) configuration, while other configurations are defined as virtual excitations with respect to it. H and L denote HOMO and LUMO orbitals, while the degenerate orbitals are denoted by additional subscripts 1, 2 etc. In parentheses next to each configuration, its coefficient in the CI expansion is indicated. Below, GS does not indicate a peak, rather it denotes the ground states wave function of the isomer. All transitions correspond to photons polarized perpendicular to the plane of the chain.

Peak	E (eV)	f	Wave function																												
GS			$ HF\rangle(0.8367)$ $ H \rightarrow L; H \rightarrow L\rangle(0.2095)$																												
I	2.42	0.0170	$ H - 1 \rightarrow L + 2\rangle(0.6840)$ $ H \rightarrow L; H - 1 \rightarrow L\rangle(0.4107)$																												
II	3.59	0.0932	$ H \rightarrow L + 4\rangle(0.6707)$ $ H - 2 \rightarrow L + 1\rangle(0.3854)$																												
III	4.07	0.1111	$ H - 5 \rightarrow L + 1\rangle(0.3510)$ $ H \rightarrow L; H \rightarrow L + 1\rangle(0.3505)$		4.14	0.0387	$ H - 5 \rightarrow L + 1\rangle(0.6436)$ $ H \rightarrow L; H - 7 \rightarrow L + 1\rangle(0.2097)$	IV	4.80	0.1128	$ H \rightarrow L + 1; H - 1 \rightarrow L + 1\rangle(0.6009)$ $ H \rightarrow L + 6\rangle(0.5196)$		4.93	0.0627	$ H - 5 \rightarrow L + 3\rangle(0.7141)$ $ H \rightarrow L + 2; H - 5 \rightarrow L + 3\rangle(0.2418)$	V	5.88	0.0077	$ H \rightarrow L + 1; H - 1 \rightarrow L + 3\rangle(0.4496)$ $ H \rightarrow L + 5; H \rightarrow L + 1\rangle(0.2934)$	VI	6.22	0.0153	$ H \rightarrow L + 2; H - 2 \rightarrow L + 1\rangle(0.2964)$ $ H - 7 \rightarrow L + 4\rangle(0.2713)$		6.45	0.0548	$ H \rightarrow L + 1; H - 2 \rightarrow L + 2\rangle(0.3201)$ $ H \rightarrow L; H - 7 \rightarrow L + 3\rangle(0.2747)$		6.68	0.0381	$ H \rightarrow L + 1; H - 2 \rightarrow L + 2\rangle(0.2930)$ $ H \rightarrow L + 2; H \rightarrow L + 4\rangle(0.2453)$
	4.14	0.0387	$ H - 5 \rightarrow L + 1\rangle(0.6436)$ $ H \rightarrow L; H - 7 \rightarrow L + 1\rangle(0.2097)$	IV	4.80	0.1128	$ H \rightarrow L + 1; H - 1 \rightarrow L + 1\rangle(0.6009)$ $ H \rightarrow L + 6\rangle(0.5196)$		4.93	0.0627	$ H - 5 \rightarrow L + 3\rangle(0.7141)$ $ H \rightarrow L + 2; H - 5 \rightarrow L + 3\rangle(0.2418)$	V	5.88	0.0077	$ H \rightarrow L + 1; H - 1 \rightarrow L + 3\rangle(0.4496)$ $ H \rightarrow L + 5; H \rightarrow L + 1\rangle(0.2934)$	VI	6.22	0.0153	$ H \rightarrow L + 2; H - 2 \rightarrow L + 1\rangle(0.2964)$ $ H - 7 \rightarrow L + 4\rangle(0.2713)$		6.45	0.0548	$ H \rightarrow L + 1; H - 2 \rightarrow L + 2\rangle(0.3201)$ $ H \rightarrow L; H - 7 \rightarrow L + 3\rangle(0.2747)$		6.68	0.0381	$ H \rightarrow L + 1; H - 2 \rightarrow L + 2\rangle(0.2930)$ $ H \rightarrow L + 2; H \rightarrow L + 4\rangle(0.2453)$				
IV	4.80	0.1128	$ H \rightarrow L + 1; H - 1 \rightarrow L + 1\rangle(0.6009)$ $ H \rightarrow L + 6\rangle(0.5196)$		4.93	0.0627	$ H - 5 \rightarrow L + 3\rangle(0.7141)$ $ H \rightarrow L + 2; H - 5 \rightarrow L + 3\rangle(0.2418)$	V	5.88	0.0077	$ H \rightarrow L + 1; H - 1 \rightarrow L + 3\rangle(0.4496)$ $ H \rightarrow L + 5; H \rightarrow L + 1\rangle(0.2934)$	VI	6.22	0.0153	$ H \rightarrow L + 2; H - 2 \rightarrow L + 1\rangle(0.2964)$ $ H - 7 \rightarrow L + 4\rangle(0.2713)$		6.45	0.0548	$ H \rightarrow L + 1; H - 2 \rightarrow L + 2\rangle(0.3201)$ $ H \rightarrow L; H - 7 \rightarrow L + 3\rangle(0.2747)$		6.68	0.0381	$ H \rightarrow L + 1; H - 2 \rightarrow L + 2\rangle(0.2930)$ $ H \rightarrow L + 2; H \rightarrow L + 4\rangle(0.2453)$								
	4.93	0.0627	$ H - 5 \rightarrow L + 3\rangle(0.7141)$ $ H \rightarrow L + 2; H - 5 \rightarrow L + 3\rangle(0.2418)$	V	5.88	0.0077	$ H \rightarrow L + 1; H - 1 \rightarrow L + 3\rangle(0.4496)$ $ H \rightarrow L + 5; H \rightarrow L + 1\rangle(0.2934)$	VI	6.22	0.0153	$ H \rightarrow L + 2; H - 2 \rightarrow L + 1\rangle(0.2964)$ $ H - 7 \rightarrow L + 4\rangle(0.2713)$		6.45	0.0548	$ H \rightarrow L + 1; H - 2 \rightarrow L + 2\rangle(0.3201)$ $ H \rightarrow L; H - 7 \rightarrow L + 3\rangle(0.2747)$		6.68	0.0381	$ H \rightarrow L + 1; H - 2 \rightarrow L + 2\rangle(0.2930)$ $ H \rightarrow L + 2; H \rightarrow L + 4\rangle(0.2453)$												
V	5.88	0.0077	$ H \rightarrow L + 1; H - 1 \rightarrow L + 3\rangle(0.4496)$ $ H \rightarrow L + 5; H \rightarrow L + 1\rangle(0.2934)$	VI	6.22	0.0153	$ H \rightarrow L + 2; H - 2 \rightarrow L + 1\rangle(0.2964)$ $ H - 7 \rightarrow L + 4\rangle(0.2713)$		6.45	0.0548	$ H \rightarrow L + 1; H - 2 \rightarrow L + 2\rangle(0.3201)$ $ H \rightarrow L; H - 7 \rightarrow L + 3\rangle(0.2747)$		6.68	0.0381	$ H \rightarrow L + 1; H - 2 \rightarrow L + 2\rangle(0.2930)$ $ H \rightarrow L + 2; H \rightarrow L + 4\rangle(0.2453)$																
VI	6.22	0.0153	$ H \rightarrow L + 2; H - 2 \rightarrow L + 1\rangle(0.2964)$ $ H - 7 \rightarrow L + 4\rangle(0.2713)$		6.45	0.0548	$ H \rightarrow L + 1; H - 2 \rightarrow L + 2\rangle(0.3201)$ $ H \rightarrow L; H - 7 \rightarrow L + 3\rangle(0.2747)$		6.68	0.0381	$ H \rightarrow L + 1; H - 2 \rightarrow L + 2\rangle(0.2930)$ $ H \rightarrow L + 2; H \rightarrow L + 4\rangle(0.2453)$																				
	6.45	0.0548	$ H \rightarrow L + 1; H - 2 \rightarrow L + 2\rangle(0.3201)$ $ H \rightarrow L; H - 7 \rightarrow L + 3\rangle(0.2747)$		6.68	0.0381	$ H \rightarrow L + 1; H - 2 \rightarrow L + 2\rangle(0.2930)$ $ H \rightarrow L + 2; H \rightarrow L + 4\rangle(0.2453)$																								
	6.68	0.0381	$ H \rightarrow L + 1; H - 2 \rightarrow L + 2\rangle(0.2930)$ $ H \rightarrow L + 2; H \rightarrow L + 4\rangle(0.2453)$																												

4. Atomic Coordinates

In this section we present tables containing the atomic coordinates, in Å units, of various isomers studied in this work.

4.1. Quasi-planar

Atom	x	y	z
B	0.854596	0.493401	0.396007
B	-0.854596	0.493401	0.396007
B	0.000000	-0.986802	0.396007
B	0.000000	2.063378	-0.045471
B	1.786937	-1.031689	-0.045471
B	-1.786937	-1.031689	-0.045471
B	2.425806	0.485458	-0.175268
B	1.633322	1.858081	-0.175268
B	-1.633322	1.858081	-0.175268
B	-2.425806	0.485458	-0.175268
B	-0.792484	-2.343538	-0.175268
B	0.792484	-2.343538	-0.175268

Table S5: Optimized coordinates of Quasi-planar (C_{3v}) isomer

4.2. Double ring

Atom	x	y	z
B	0.000000	1.645803	0.755665
B	-1.425308	0.822902	0.755665
B	-1.425308	-0.822902	0.755665
B	0.000000	-1.645803	0.755665
B	1.425308	-0.822902	0.755665
B	1.425308	0.822902	0.755665
B	0.822902	1.425308	-0.755665
B	1.645803	0.000000	-0.755665
B	0.822902	-1.425308	-0.755665
B	-0.822902	-1.425308	-0.755665
B	-1.645803	0.000000	-0.755665
B	-0.822902	1.425308	-0.755665

Table S6: Optimized coordinates of Double ring (D_{6d}) isomer

4.3. Chain

Atom	x	y	z
B	-0.430275	4.400542	0.000000
B	0.905913	3.618456	0.000000
B	-0.755353	2.873999	0.000000
B	0.914514	2.038590	0.000000
B	-0.777694	1.210978	0.000000
B	0.755353	0.376209	0.000000
B	-0.755353	-0.376209	0.000000
B	0.777694	-1.210978	0.000000
B	-0.914514	-2.038590	0.000000
B	0.755353	-2.873999	0.000000
B	-0.905913	-3.618456	0.000000
B	0.430275	-4.400542	0.000000

Table S7: Optimized coordinates of Chain (C_{2h}) isomer

4.4. Hexagons

Atom	x	y	z
B	0.000000	0.000000	0.844921
B	0.000000	1.517663	0.000000
B	0.000000	-1.517663	0.000000
B	0.000000	-1.664249	1.586458
B	0.000000	-0.768140	2.882657
B	0.000000	0.768140	2.882657
B	0.000000	1.664249	1.586458
B	0.000000	0.000000	-0.844921
B	0.000000	-0.768140	-2.882657
B	0.000000	0.768140	-2.882657
B	0.000000	1.664249	-1.586458
B	0.000000	-1.664249	-1.586458

Table S8: Optimized coordinates of Hexagons (D_{2h}) isomer

4.5. Quad

Atom	x	y	z
B	0.000000	2.015258	0.000000
B	0.000000	0.000000	1.268281
B	0.000000	0.000000	-1.268281
B	0.000000	-2.015258	0.000000
B	-1.682909	0.000000	-0.912871
B	-1.490298	-1.389700	0.000000
B	-1.490298	1.389700	0.000000
B	-1.682909	0.000000	0.912871
B	1.682909	0.000000	0.912871
B	1.490298	-1.389700	0.000000
B	1.490298	1.389700	0.000000
B	1.682909	0.000000	-0.912871

Table S9: Optimized coordinates of Quad (D_{2h}) isomer

4.6. Pris-3-square-1

Atom	x	y	z
B	0.000000	1.574917	0.000000
B	1.574917	0.000000	0.000000
B	-1.574917	0.000000	0.000000
B	0.000000	-1.574917	0.000000
B	-0.862562	0.862562	1.264540
B	-0.862562	-0.862562	1.264540
B	0.862562	0.862562	1.264540
B	0.862562	-0.862562	1.264540
B	0.862562	0.862562	-1.264540
B	0.862562	-0.862562	-1.264540
B	-0.862562	0.862562	-1.264540
B	-0.862562	-0.862562	-1.264540

Table S10: Optimized coordinates of Pris-3-square-1 (D_{4h}) isomer

4.7. *Pris-3-square-2*

Atom	x	y	z
B	0.000000	1.870473	0.000000
B	1.870473	0.000000	0.000000
B	-1.870473	0.000000	0.000000
B	0.000000	-1.870473	0.000000
B	-0.896666	0.896666	0.994197
B	-0.896666	-0.896666	0.994197
B	0.896666	0.896666	0.994197
B	0.896666	-0.896666	0.994197
B	0.896666	0.896666	-0.994197
B	0.896666	-0.896666	-0.994197
B	-0.896666	0.896666	-0.994197
B	-0.896666	-0.896666	-0.994197

Table S11: Optimized coordinates of Pris-3-square-2 (D_{4h}) isomer

4.8. *Parallel triangular*

Atom	x	y	z
B	0.000000	1.069852	0.924715
B	-0.926519	-0.534926	0.924715
B	0.926519	-0.534926	0.924715
B	0.000000	1.069852	-0.924715
B	0.926519	-0.534926	-0.924715
B	-0.926519	-0.534926	-0.924715
B	0.000000	0.989584	2.529660
B	-0.857005	-0.494792	2.529660
B	0.857005	-0.494792	2.529660
B	0.000000	0.989584	-2.529660
B	0.857005	-0.494792	-2.529660
B	-0.857005	-0.494792	-2.529660

Table S12: Optimized coordinates of Parallel triangular (D_{3h}) isomer

4.9. *Planar square*

Atom	x	y	z
B	0.000000	1.237919	0.000000
B	1.237919	0.000000	0.000000
B	-1.237919	0.000000	0.000000
B	0.000000	-1.237919	0.000000
B	-1.237919	2.340594	0.000000
B	1.237919	2.340594	0.000000
B	2.340594	1.238828	0.000000
B	2.340594	-1.238828	0.000000
B	-2.340594	-1.238828	0.000000
B	-2.340594	1.238828	0.000000
B	1.238828	-2.340594	0.000000
B	-1.238828	-2.340594	0.000000

Table S13: Optimized coordinates of Planar square (D_{4h}) isomer

4.10. Perfect Icosahedron

Atom	x	y	z
B	0.000000	0.865000	1.399599
B	0.000000	0.865000	-1.399599
B	0.000000	-0.865000	1.399599
B	0.000000	-0.865000	-1.399599
B	1.399599	0.000000	0.865000
B	-1.399599	0.000000	0.865000
B	1.399599	0.000000	-0.865000
B	-1.399599	0.000000	-0.865000
B	0.865000	1.399599	0.000000
B	0.865000	-1.399599	0.000000
B	-0.865000	1.399599	0.000000
B	-0.865000	-1.399599	0.000000

Table S14: Optimized coordinates of perfect Icosahedron (I_h) isomer

4.11. Distorted Icosahedron

Atom	x	y	z
B	0.000000	0.852920	-1.337059
B	0.000000	0.852920	1.337059
B	0.000000	-0.852920	-1.337059
B	0.000000	-0.852920	1.337059
B	-1.394554	0.000000	-0.843230
B	1.394554	0.000000	-0.843230
B	-1.394554	0.000000	0.843230
B	1.394554	0.000000	0.843230
B	-0.897896	1.466072	0.000000
B	-0.897896	-1.466072	0.000000
B	0.897896	1.466072	0.000000
B	0.897896	-1.466072	0.000000

Table S15: Optimized coordinates of distorted Icosahedron (D_{2h}) isomer

5. Nature of the Wave Function of the Lowest Singlet State of B_{12} Icosahedron

We performed calculations on the lowest singlet state of the B_{12} isomer with perfect icosahedral symmetry (I_h), by employing multi-reference singles-doubles CI (MRSDCI) level of theory, and cc-pVDZ basis set, to understand the nature of its wave function. For the purpose we used the HF orbitals, and the seven reference configurations listed in the table below. From the magnitudes of the coefficients of the reference configurations in the CI expansion of the wave function, it is obvious that the closed-shell HF reference state dominates the wave function. Therefore, any single-reference approach such as CCSD, using the HF state as the reference, will give reasonable results for this state.

Table S16: Many-particle wave function of the lowest singlet state of isomer of B_{12} with perfect icosahedral symmetry (I_h) (Fig. 1e of the main article). $|HF\rangle$ indicates the closed-shell Hartree-Fock (HF) configuration, while other configurations are defined as virtual excitations with respect to it. H and L denote HOMO and LUMO orbitals. In the parentheses next to each configuration, its coefficient in the CI expansion is indicated.

Dominant configurations in the MRSDCI wave function	
$ HF\rangle$	(0.8097)
$ H \rightarrow L + 3; H \rightarrow L + 3\rangle$	(0.2697)
$ H \rightarrow L + 3; H - 1 \rightarrow L + 6\rangle$	(0.1444)
$ H \rightarrow L + 2; H - 1 \rightarrow L + 3\rangle$	(0.1339)
$ H \rightarrow L + 3; H - 2 \rightarrow L + 3\rangle$	(0.1049)
$ H \rightarrow L + 3; H - 8 \rightarrow L + 1\rangle$	(0.0922)
$ H - 1 \rightarrow L + 4; H - 3 \rightarrow L + 6\rangle$	(0.0901)